Carbon nanostraws: nanotubes filled with superparamagnetic nanoparticles

2009 Nanotechnology 20 485604

(http://iopscience.iop.org/0957-4484/20/48/485604)

Nanotechnology **20** (2009) 485604 (7pp) doi:10.1088/0957-4484/20/48/485604

Carbon nanostraws: nanotubes filled with superparamagnetic nanoparticles

Susmita Pal, Sayan Chandra, Manh-Huong Phan, Pritish Mukherjee and Hariharan Srikanth[1]

Integrated Functional Materials Group, Department of Physics, University of South Florida, Tampa, FL 33620, USA

E-mail: sharihar@cas.usf.edu

Received 20 July 2009, in final form 13 October 2009
Published 30 October 2009
Online at stacks.iop.org/Nano/20/485604

Abstract

A two-step magnetically assisted capillary action method is demonstrated as a facile technique to produce hollow carbon nanotubes filled with uniformly dispersed Fe_3O_4 nanoparticles (NPs). Template-assisted chemical vapor deposition (CVD) grown CNTs with average diameter 200–300 nm and length 5–6 μm were effectively used as 'nanostraws' to suck in chemically synthesized Fe_3O_4 nanoparticles (mean size ~6 nm) in a ferrofluid suspension. Temperature and magnetic field-dependent DC magnetization measurements indicate that these functionalized nanotubes are superparamagnetic at room temperature with enhanced interparticle interactions due to the close packing of the nanoparticles within the tubes. Magnetic relaxation phenomena in these filled nanotubes are probed using frequency-dependent AC susceptibility. The reasonably large saturation magnetization ($M_s = 65$ emu g^{-1}) attained in these nanostructures makes them very promising for a diverse set of applications that utilize both the magnetic and dielectric functionalities of these composite nanotube materials.

1. Introduction

In recent years, carbon nanotubes (CNTs) have been used in many potential applications including nano-devices, sensors, ultrahigh strength engineered fibers, quantum wires, and catalyst supports [1–7]. Bio-functionalized CNTs have recently been tested for tumor targeting applications with reduced toxicity [8, 9]. Computer simulation results predicted that fullerene tubules may act as molecular straws which are capable of absorbing polar molecules by capillary action [10]. Consequently, a number of methods have been developed to fill CNTs with various kinds of materials including metals, non-metals, and oxides [11–14]. Recent studies have been focused on the synthesis of high aspect ratio magnetic materials using porous templates. Among these, anodic alumina templates and multi-walled carbon nanotube templates are of note [15, 16]. In particular, CNTs have been used as a promising template for fabricating CNT based metal, metal oxide, or metal nitride nanorods with higher selectivity which possess unique physical, chemical, and mechanical properties [17–19]. Recently, it has been reported that Fe_3O_4 filled CNTs may be used as diffraction gratings, optical filters, and polarizers [20]. Other applications of these materials include cantilever tips in magnetic force microscopes, magnetic stirrers or magnetic valves in nanofluidic devices [20]. Also, well-defined CNTs embedded with superparamagnetic nanoparticles (for example, Fe_3O_4) can be used in magnetic sensing. Korneva *et al* proposed that these magnetically filled CNTs can potentially be used as nanosubmarines driven through blood vessels by an external magnetic field and transporting drugs to specific locations in the body, as well as for medical diagnosis without surgical interference [17]. Since the biocompatibility of magnetite and CNTs is quite well established in the literature [21, 22], the combination of these two nanostructured elements could be of potential interest for improved drug delivery systems. There is also considerable interest in high aspect ratio magnetic nanostructures where the anisotropy can be tuned easily compared to as-synthesized magnetic colloids. To realize such applications, it is technologically important to retain the desirable magnetic properties of magnetic nanoparticles in CNTs through control over the particle size and uniformity of packed particles. Despite a number of previous studies, filling CNTs completely with monodisperse Fe_3O_4 nanoparticles has remained a challenging task. Moreover, it is essential to understand the magnetic

[1] Author to whom any correspondence should be addressed.

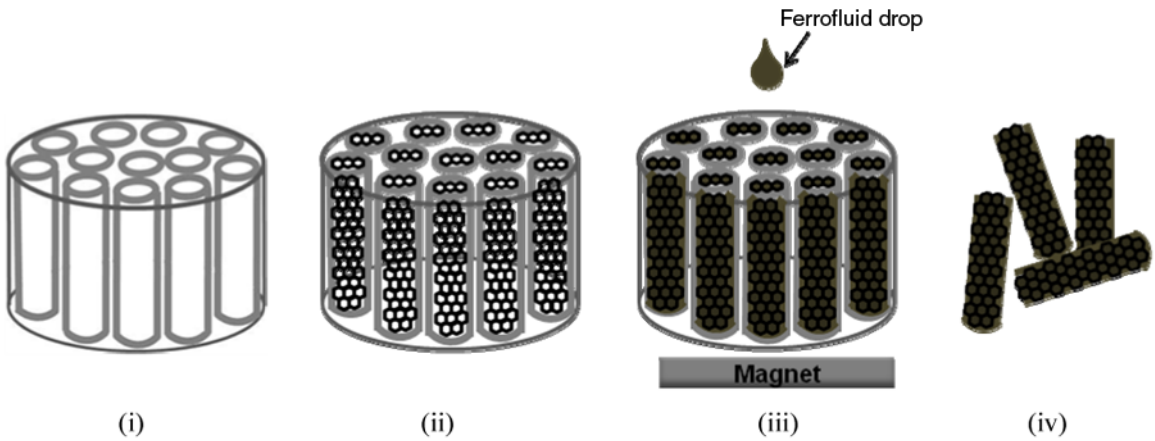

Figure 1. Scheme of the synthesis steps: (i) alumina template, (ii) CNT grown by the CVD technique inside the template, (iii) CNTs filled by ferrofluids dropwise keeping a magnet underneath the template, (iv) CNTs filled with ferrofluid after removing the template.

interactions that are likely to influence the magnetic properties of Fe_3O_4-filled CNTs.

In this paper, we present the synthesis, structural, and magnetic properties of hollow, straw-like CNTs (open at both ends) filled with the Fe_3O_4 nanoparticles. A facile, multi-step process was utilized to fabricate these structures. First we synthesized the magnetite nanoparticles chemically, and separately used chemical vapor deposition (CVD) to grow multi-walled CNTs within the pores of alumina templates. The Fe_3O_4 NPs were incorporated inside the CNTs using a magnetically assisted capillary action method [17]. We demonstrate that the optimization of loading conditions in a magnetically assisted capillary action technique allows production of CNTs filled completely with uniformly dispersed Fe_3O_4 nanoparticles and that the increased dipolar interparticle interaction leads to the enhanced magnetic properties of these nanostructures. Detailed magnetic characterization was performed using DC and AC susceptibility experiments. To our knowledge this is the first report of uniformly filled CNTs displaying large saturation magnetization which would render them useful for various applications.

2. Experimental details

We now describe the multi-step process involved in the fabrication of magnetic nanoparticle loaded carbon nanotubes. The entire process consisted of three different steps (figure 1): (i) synthesis of Fe_3O_4 nanoparticles; (ii) carbon nanotubes grown by the CVD technique; (iii) filling of the carbon nanotubes by as-prepared Fe_3O_4 nanoparticles.

2.1. Synthesis of Fe_3O_4 nanoparticles

The nearly spherical Fe_3O_4 nanoparticles were synthesized using the procedure introduced by Sun *et al* [23]. Briefly, 2 mmol iron (III) acetylacetonate ($Fe(acac)_3$), 10 mmol 1,2-hexadecanediol, 6 mmol oleic acid, 6 mmol oleylamine, 20 ml benzyl ether were mixed together and magnetically stirred under the flow of argon at 200 °C for 2 h. Then the mixture was heated to reflux at 300 °C for 1 h. The black colored material was cooled down to room temperature. 40 ml ethanol was added to the mixture and the precipitate was separated by centrifugation. The product was dissolved in hexane in the presence of oleic acid and oleylamine. This solution was centrifuged to remove the undispersed residue. The product was precipitated again with ethanol and centrifuged to remove the solvent and was finally dissolved in hexane for further characterization.

2.2. Synthesis of carbon nanotubes

Carbon nanotubes were produced using a chemical vapor deposition (CVD) method and directly grown inside the pores of alumina membranes. The procedure was similar to that reported by Miller *et al* [24]. Before the growth of CNTs, the alumina template membranes were placed between two quartz slides and heated to 740 °C for 1 h to prevent the bending of templates during the CNT synthesis. The heat-treated alumina template membrane (13 mm diameter, 60 μm thick, and 0.2 μm pore size purchased from Whatman) was placed vertically inside the quartz tube. The quartz tube loaded with the alumina template was placed inside the CVD reactor furnace and its temperature was increased to 670 °C under the flow of argon (flow rate 20 sccm). When the temperature stabilized at 670 °C, the gas flow was switched to 30% ethylene and 70% helium at a flow rate of 20 sccm. The reaction was continued for 6 h and the gas flow was switched back to argon at a flow rate of 20 sccm. The furnace was turned off and allowed to cool down to room temperature still maintaining the flow of argon. Note that while attempts were made to use alumina with smaller pore size as quoted by the manufacturers, the nanotubes grown were on average much larger (in the 250–300 nm range). This is most likely due to the pore size not being uniform through the depth of the 60 μm thick alumina templates.

2.3. Filling the CNTs with Fe_3O_4 nanoparticles

The next step was filling the carbon nanotubes (open at both ends) encased in the alumina templates with the organic solvent

containing the suspended Fe_3O_4 nanoparticles. Before filling the nanotubes, a permanent magnet ($\mu_0 H = 0.4$ T) was placed underneath the template and the hexane solution of Fe_3O_4 was poured dropwise on the top end of the template. The ferrofluid invaded the pores due to capillary action and the homogeneous magnetic field helped to increase the rate and depth of penetration. After the evaporation of hexane at room temperature, the template was broken into tiny pieces and dipped into 4.0 M NaOH solution and sonicated until the template dissolved completely. After sonication, the solution was vacuum filtered through a polyester nucleopore membrane (pore size ∼0.2 μm). After filtration, the residue was rinsed with toluene to remove the stray ferrofluid particles from the surface of the membrane. Then the residue was washed with isopropanol and deionized water several times and finally dried at room temperature. The dry sample was collected for structural characterization and magnetic measurements.

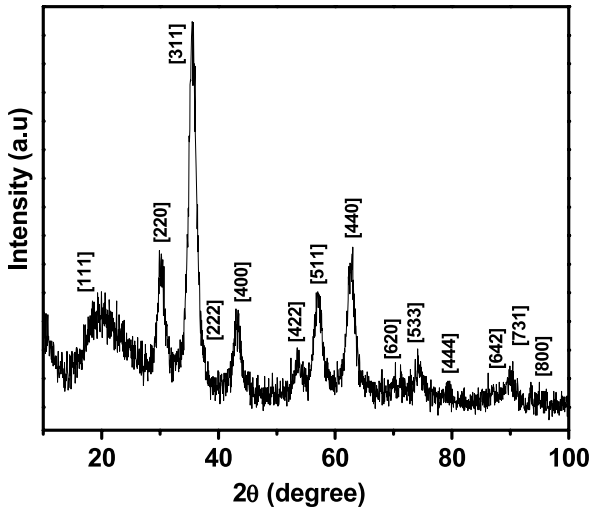

Figure 2. XRD pattern of 6 nm Fe_3O_4 nanoparticles.

3. Structural characterization

The inverse spinel crystal structure of magnetite was confirmed by x-ray powder diffraction using a Phillips diffractometer with a Cu Kα source. The size and shape of iron oxide nanoparticles and the nanoparticle filled CNTs were characterized using a Morgagni transmission electron microscope (TEM). For TEM characterization, the iron oxide nanoparticles suspended in hexane and iron oxide loaded CNTs suspended in isopropanol were drop cast on a carbon coated Cu grid.

4. Magnetic characterization

Standard magnetic measurements such as the temperature dependence of zero-field-cooled (ZFC) and field-cooled (FC) susceptibility, M–H hysteresis loop measurements, and AC susceptibility were carried out using a commercial Physical Property Measurement System (PPMS) from Quantum Design (San Diego, CA) over a wide range of temperatures and magnetic fields. For all the measurements, the dry samples were loaded in a standard, non-magnetic gelatin capsule.

5. Results and discussion

The experimental procedure of Fe_3O_4 NP filled CNTs is illustrated schematically in figure 1, and the resulting structures are shown in figures 2 and 3. Figure 2 shows the XRD pattern of Fe_3O_4 nanoparticles and the peaks are consistent with the expected inverse spinel crystal structure.

TEM images of Fe_3O_4 nanoparticles and Fe_3O_4 loaded CNTs are shown in figure 3. The average particle size of Fe_3O_4 was estimated from a histogram analysis to be 6 ± 0.5 nm (figure 3(a)). Several different views of the nanoparticle loaded CNTs are shown in figures 3(b)–(d). It can be seen that the particle packing within the cross-section of the nanotubes is very uniform. The average length of CNT is 5–6 μm and the diameter is 250–300 nm with 30 nm wall thickness. So the aspect ratio of these magnetic nanotubes turns out to be ∼20. These dimensions are determined by the commercial alumina templates used in the CVD growth. Figure 3(b) shows that there are well-defined regions within long nanotubes in which the nanoparticle packing is either dense or relatively sparse, respectively, giving it a bamboo shoot like appearance. Since the suction of the fluid with nanoparticles into the nanotubes is governed by magnetically assisted capillary action, this feature can be reconciled as due to variable surface tension and adhesive properties of the inner wall of the nanotubes. CVD-grown nanotubes have been known to have variable internal stress distributions that act as nucleation centers for accumulation of defects or inclusions [25]. It is worth mentioning here that the other figures 3(c) and (d) show that a high degree of uniformity in filling can be achieved over lengths of the order of 1 μm.

Figure 4 shows the zero-field-cooled (ZFC) and field-cooled (FC) DC magnetization curves for Fe_3O_4 NPs and CNTs filled with Fe_3O_4 NPs (labeled as Fe_3O_4-CNTs) taken at a field of 200 Oe. The ZFC curve for Fe_3O_4 NPs exhibits the typical blocking process of an assembly of superparamagnetic particles with a distribution in blocking temperature around an average $T_B \sim 31$ K. The proximity of the ZFC peak and the onset temperature of the irreversibility between the ZFC and FC magnetization curves are signatures of monodisperse nature and clearly exclude a large extent of particle aggregation or a large size distribution, which is consistent with the TEM characterization of the samples (see figure 3(a)). However, the case is quite different for Fe_3O_4-CNTs, which exhibit a broad ZFC curve with its peak at ∼58 K. For this sample, the gradual decrease in magnetization above 58 K, deviating from Curie type $1/T$ dependence, is characteristic of the presence of particle interactions in this system [26].

Figures 5(a) and (b) and its insets show the magnetic-field dependence of magnetization (the M–H curves) taken at 5 and 300 K. It can be observed that for both Fe_3O_4 NPs and Fe_3O_4-CNTs the M–H curves at 300 K do not show any hysteresis, whereas a clear hysteresis with a coercivity of $H_C \sim 25$ Oe for Fe_3O_4 NPs and $H_C \sim 140$ Oe for Fe_3O_4-CNTs are observed at 5 K. This is characteristic of the sample being superparamagnetic at room temperature and entering a blocked state at low temperature which results in opening up of

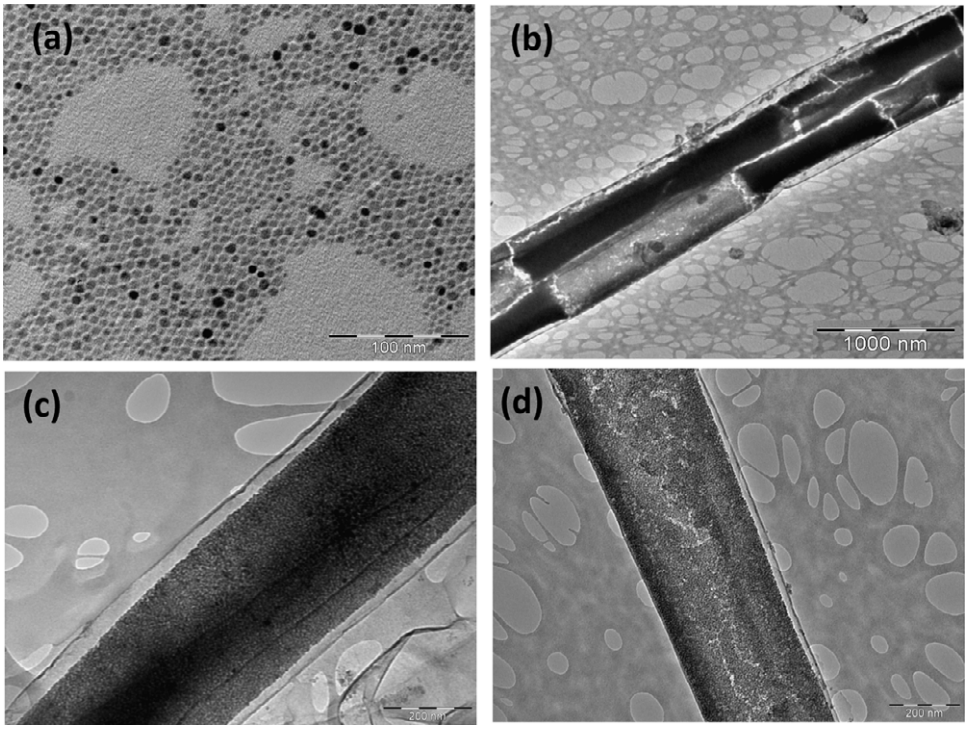

Figure 3. TEM micrographs of (a) Fe_3O_4 nanoparticles and (b)–(d) carbon nanotubes filled with Fe_3O_4 nanoparticles.

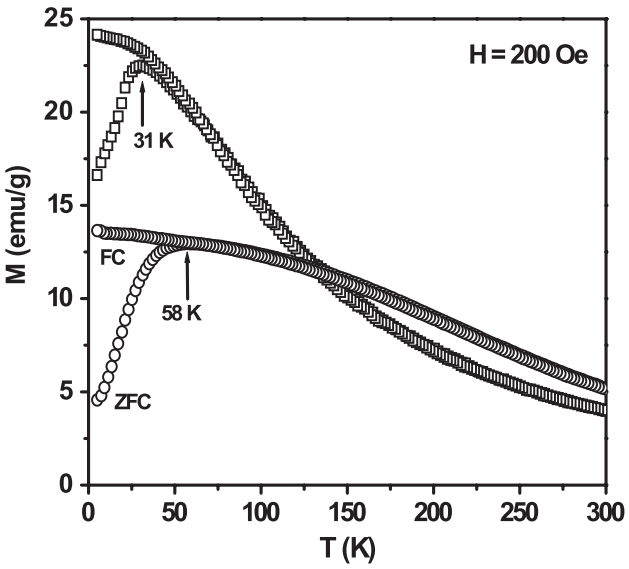

Figure 4. M versus T plot of Fe_3O_4 nanoparticles (□) and carbon nanotubes filled with Fe_3O_4 nanoparticles (○).

the hysteresis loop. As compared with Fe_3O_4 NPs, a slightly non-saturated magnetization feature at low magnetic fields is observed for Fe_3O_4-CNTs, which is attributed to the stronger particle interaction present in this sample, as demonstrated below. At 5 K the values of saturation magnetization (M_s) of Fe_3O_4 NPs and Fe_3O_4-CNTs are determined to be $\sim$60 emu g^{-1} and $\sim$65.3 emu g^{-1}, respectively. It should be noted that the saturation magnetization for the Fe_3O_4-CNT system is estimated using the total mass of the sample as is commonly reported in the literature for composite systems [27, 28]. Thus the M_s value is the lower limit and would be slightly higher if we consider the mass of Fe_3O_4 content only. To estimate the weight of CNT only in the Fe_3O_4-CNT system, we used a high resolution balance and separately weighed the Fe_3O_4 nanoparticles, composites, and CNTs taking care that they were the same quantities used in the magnetic measurements. The contribution of CNT was 43 times smaller (0.15 mg) with respect to the weight of Fe_3O_4 (6.3 mg) of the sample. Likodimos *et al* [29] have shown that pure CNTs exhibit a diamagnetic behavior with $M = -0.7$ emu g^{-1} at an applied field of 50 kOe. Subtracting the diamagnetic contribution of CNTs, the M_s of Fe_3O_4-CNTs is $\sim$64.6 emu g^{-1}. This value is smaller than that of bulk Fe_3O_4 ($M_s \sim 92$ emu g^{-1}) but is larger than that of Fe_3O_4 NPs ($M_s \sim$ 60 emu g^{-1}). The increase in saturation magnetization we observe is consistent with other reports in the literature [27, 28] for maghemite and magnetite nanoparticles attached to the external surface of CNTs. The enhancement of M_s for Fe_3O_4-CNTs is very important from the magnetic-field guided applications point of view. In fact, a significant reduction of M_s observed in Fe_3O_4 nanoparticles coated with gold or CdSe is the major obstacle for biomedical application of these systems [30, 31]. Note that since there is no high temperature annealing or treatment involved in filling the nanotubes with magnetite nanoparticles, there is no interaction between the components at the inner walls of the nanotubes. This is verified through structural characterization which shows no evidence for cementite phase (Fe_3C) formation. Thus we believe that our facile synthesis route aids in retention of the large saturation magnetization. The slight enhancement of the magnetization in the Fe_3O_4-CNT system in comparison with

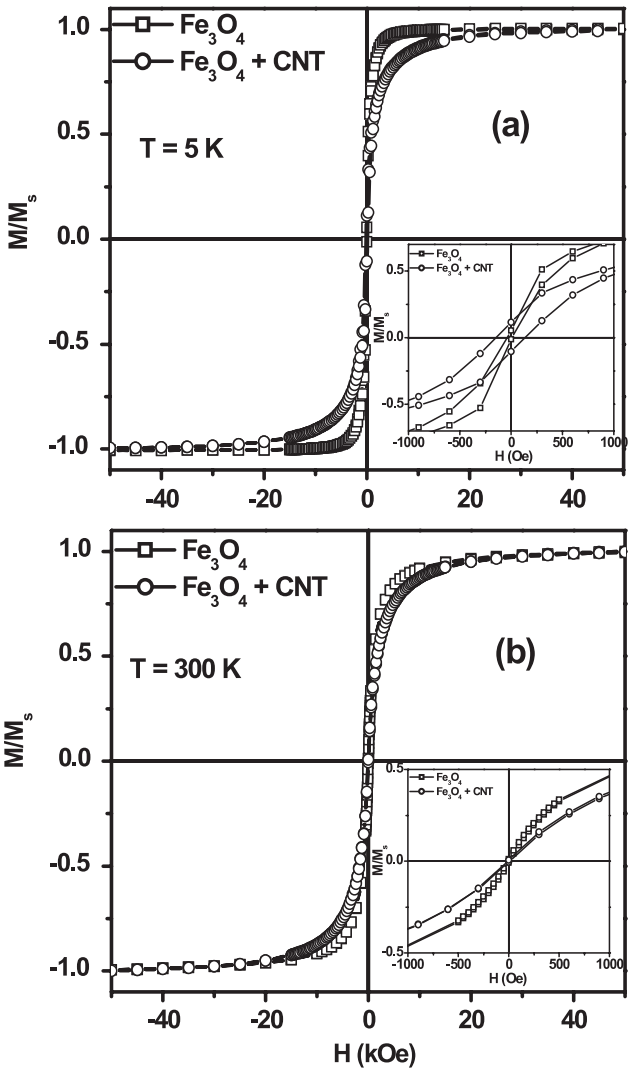

Figure 5. M versus H plot of Fe_3O_4 nanoparticles (□) and carbon nanotubes filled with Fe_3O_4 nanoparticles (○) at (a) 5 K and (b) 300 K. ($M_s = 60$ emu g^{-1} for Fe_3O_4 NPs and 64.6 emu g^{-1} for carbon nanotube filled Fe_3O_4 NPs)

the as-synthesized Fe_3O_4 nanoparticles is also consistent with enhanced interparticle interactions (due to tight packing of the particles within the confined region of the hollow nanotubes) that is discussed and quantitatively analyzed in the following section.

It is generally accepted that the magnetic interactions that dominate in magnetic nanoparticle assemblies are dipole–dipole interparticle interactions (which are always present) and exchange interactions through the surfaces of particles that are in close contact [26, 31]. In the present case, the exchange interaction among Fe_3O_4 particles might be minimal because the average edge–edge separation between particles is large due to the presence of the surfactant [26]. However, the tight packing of Fe_3O_4 NPs inside CNTs can reduce the average distance between Fe_3O_4 particles, thus enhancing the strength of the dipolar interparticle interaction. Recently, our group has demonstrated the effect of the dipolar interaction on the magnetic parameters in 3D soft ferrite nanoparticle assemblies [32]. It has been shown that the stronger the dipolar interparticle interaction, the higher the blocking temperature (T_B) and coercivity (H_C). This leads to a similar expectation that Fe_3O_4-CNTs possess a stronger interparticle interaction, thus enhancing T_B and H_C, in comparison with Fe_3O_4 NPs.

To clarify this, we conducted AC susceptibility measurements at different frequencies, the results of which are displayed in figures 6(a) and (b). It is evident that for both the samples χ' peaks are situated at a temperature higher than that for χ'' peaks, and T_B is determined by the peak in χ'' which shifts to higher temperature as frequency is increased. This feature has also been observed in other nanoparticle assemblies [30]. Therefore, the frequency dependence of the peaks in χ'' was used to fit to both the Néel–Arrhenius model,

$$\tau = \tau_0 \exp(E_a/kT_B) \tag{1}$$

and the Volgel–Fulcher (VF) scaling law,

$$\tau = \tau_0 \exp[E_a/k(T_B - T_0)] \tag{2}$$

where τ is the relaxation time ($\tau = 1/f$; f is the frequency), τ_0 is the microscopic flipping time of the fluctuating spins, E_a is the thermal activation energy, T_B is the blocking temperature, and T_0 is the characteristic temperature with thermal energy dominating for $T > T_0$ and interaction energy for $T < T_0$.

Our results reveal that the $\chi''(T)$ data for both samples can be fit using equation (1), but the fitting parameters obtained are unphysical ($\tau_0 = 1.49 \times 10^{-14}$ s and $E_a/k = 1003$ K for Fe_3O_4 NPs and $\tau_0 = 6.48 \times 10^{-15}$ s and $E_a/k = 2141$ K for Fe_3O_4-CNTs). Meanwhile, the VF model (e.g. equation (2)) fits well the $\chi''(T)$ data (see figure 7) with acceptable fit parameters ($\tau_0 = 1.09 \times 10^{-12}$ s, $E_a/k = 698$ K, and $T_0 = 7$ K for Fe_3O_4 NPs and $\tau_0 = 4.78 \times 10^{-10}$ s, $E_a/k = 711$ K, and $T_0 = 34$ K for Fe_3O_4-CNTs). This clearly indicates that the present samples belong to the class of interacting particle systems [26, 29]. Equation (2) can also be rewritten in the other form, $T_B = T_0 + (E_a/k)/\ln(\tau/\tau_0)$. From this equation, it is evident that the magnitude of T_0 is a measure of the strength of the dipolar interparticle interaction and that the larger the value of T_0, the larger the value of T_B. Therefore, the larger value of T_0 for Fe_3O_4-CNTs clearly indicates the stronger interparticle interactions in this system. In other words, our quantitative analysis shows that the enhancement of T_B in Fe_3O_4-CNTs is the result of the increased interparticle interactions due to the dense packing nature of Fe_3O_4 NPs inside CNTs. Furthermore, we note that the effect of the dipolar interparticle interaction among Fe_3O_4 particles can also introduce a self-averaging effect over a correlation length, which results in a larger average 'magnetic' size of the apparent particles (i.e. the increased particle volume, V) [33, 34]. Since T_B is proportional to V via $E_a = KV$ (K is the anisotropy constant), the increase of V leads to the increase of T_B in Fe_3O_4-CNTs. This may also be reconciled with the fact that the increase of V enhances the magnetic relaxation time (τ) of this system. This has been supported by recent observations of the existence of multiparticle magnetic correlations in dense nanoparticle assemblies, even in the absence of an applied magnetic field [35].

An important consequence that emerges for the first time from our study is that the uniformity of highly packed Fe_3O_4

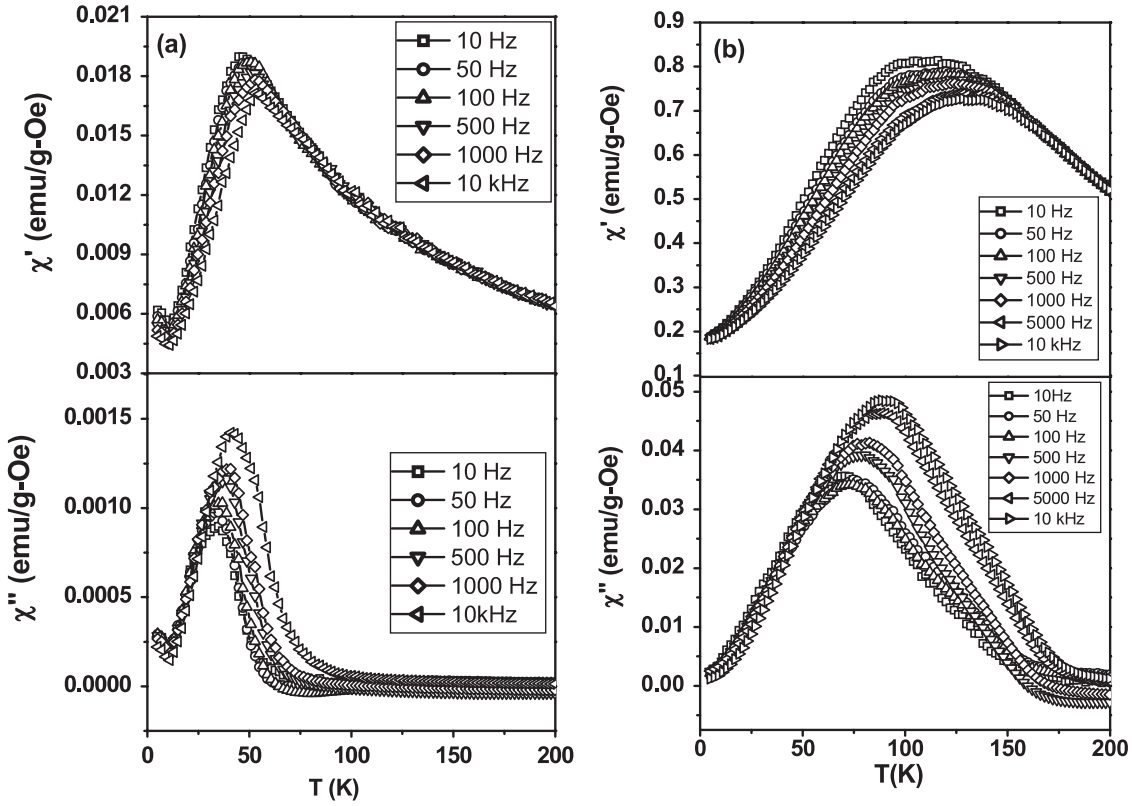

Figure 6. AC susceptibility graphs of (a) Fe_3O_4 nanoparticles and (b) carbon nanotubes filled with Fe_3O_4 nanoparticles.

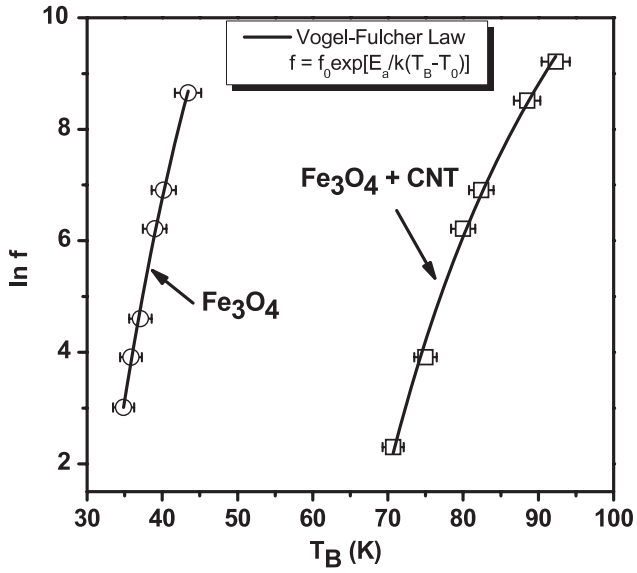

Figure 7. Volgel–Fulcher fitting data of Fe_3O_4 nanoparticles (○) and carbon nanotubes filled with Fe_3O_4 nanoparticles (□).

particles in carbon nanotubes leads to the enhancement of the dipolar interparticle interaction and hence the magnetic properties of this system. This is of practical importance in developing carbon nanotubes filled with superparamagnetic nanoparticles for a wide range of applications such as diffraction gratings, optical filters, polarizers, and magnetic sensing.

6. Conclusions

We have successfully synthesized Fe_3O_4 nanoparticle loaded carbon nanotubes with a high degree of uniformity in filling, using a magnetically assisted capillary action technique. We demonstrate that good magnetic properties are achieved in carbon nanotubes filled completely with uniformly dispersed Fe_3O_4 nanoparticles and that the increased dipolar interparticle interaction leads to the enhanced magnetic properties of these nanostructures. These results are of practical importance in developing novel magnetically filled carbon nanotubes for magnetic-field guided applications.

Acknowledgments

The authors thank Dr Garrett Matthews and Yasin al Titi for access to their laboratory and assistance with the CVD growth of carbon nanotubes. This work is supported by a grant from DoD-USAMRMC through grant number W81XWH-07-1-0708. HS also acknowledges support from NSF through GOALI grant CMMI 0728073.

References

[1] Collins P G, Zettl A, Bando H, Thess A and Smalley R E 1997 *Science* **278** 100–3
[2] Rinkiö M, Johansson A, Paraoanu G S and Törmä P 2009 *Nano Lett.* **9** 643–7
[3] Kong J, Franklin N R, Zhou C, Chapline M G, Peng S, Cho K and Dai H 2000 *Science* **287** 622–5

[4] Tans S J, Devoret M H, Dai H, Thess A, Smalley R E, Geerligs L G and Dekker C 1997 *Nature* **386** 474–7
[5] Treacy M M J, Ebbesen T W and Gibson J M 1996 *Nature* **381** 678–80
[6] Planeix J M, Coustel N, Coq B, Brotons V, Kumbhar P S, Dutartre R, Geneste P, Bernier P and Ajayan P M 1994 *J. Am. Chem. Soc.* **116** 7935–6
[7] Kim C, Kim Y A, Kim J H, Kataoka M and Endo M 2008 *Nanotechnology* **19** 145602
[8] Villa C H, McDevitt M R, Escorcia F E, Rey D A, Bergkvist M, Batt C A and Scheinberg D A 2008 *Nano Lett.* **8** 4221–8
[9] Chakravarty P, Marches R, Zimmerman N S, Swafford A D-E, Bajaj P, Musselman I H, Pantano P, Draper R K and Vitetta E S 2008 *Proc. Natl Acad. Sci. USA* **105** 8697–702
[10] Pederson M R and Broughton J Q 1992 *Phys. Rev. Lett.* **69** 2689–92
[11] Ajayan P M and Iijima S 1993 *Nature* **361** 333–34
[12] Elías A L *et al* 2005 *Nano Lett.* **5** 467–72
[13] Muramatsu H, Hayashi T, Kim A Y, Shimamoto D, Endo M, Terrons M and Dresselhaus M S 2008 *Nano Lett.* **8** 237–40
[14] Yuge R, Ichihashi T, Shimakawa Y, Kubo Y, Yudasaka M and Iijima S 2004 *Adv. Mater.* **16** 1420–3
[15] Keller N, Pham-Huu C, Shiga T, Estournès C, Grenèche J M and Ledoux M J 2004 *J. Magn. Magn. Mater.* **272–276** 1642–4
[16] Ji G, Tang S, Xu B, Gu B and Du Y 2003 *Chem. Phys. Lett.* **379** 484–89
[17] Korneva G, Ye H, Gogotsi Y, Halverson D, Friedman G, Bradley J-C and Kornev K G 2005 *Nano Lett.* **5** 879–84
[18] Ersen O, Bégin S, Houllé M, Amadou J, Janowska I, Grenèche J-M, Crucifix C and Pham-Huu C 2008 *Nano Lett.* **8** 1033–40
[19] Hu J, Bando Y, Zhan J, Zhi C and Goldberg D 2006 *Nano Lett.* **6** 1136–40
[20] Kornev K G, Halverson D, Korneva G, Gogotsi Y and Friedman G 2008 *Appl. Phys. Lett.* **92** 233117
[21] Gupta A K and Gupta M 2005 *Biomaterials* **26** 3995–4021
[22] Lu F, Gu L, Meziani M J, Wang X, Luo P G, Veca L M, Cao L and Sun Y-P 2009 *Adv. Mater.* **21** 139–52
[23] Sun S and Zeng H 2002 *J. Am. Chem. Soc.* **124** 8204–5
[24] Miller S A, Young V Y and Martin C R 2001 *J. Am. Chem. Soc.* **123** 12335–42
[25] Wei D and Liu Y 2008 *Adv. Mater.* **20** 2815–41
[26] Majetich S A and Sachan M 2006 *J. Phys. D: Appl. Phys.* **39** R407–22
[27] Correa-Duarte M A, Grzelczak M, Salgueiriño-Maceira V, Giersig M, Liz-Marzán L M, Farle M, Sierazdki K and Diaz R 2005 *J. Phys. Chem.* B **109** 19060–3
[28] Choi J H, Nguyen F T, Barone P W, Heller D A, Moll A E, Patel D, Boppart S A and Strano M S 2007 *Nano Lett.* **7** 861–7
[29] Likodimos V, Glenis S, Guskos N and Lin C L 2003 *Phys. Rev.* B **68** 045417
[30] Pal S, Morales M B, Mukherjee P and Srikanth H 2009 *J. Appl. Phys.* **105** 07B504
[31] Gao J, Zhang W, Huang P, Zhang B, Zhang X and Xu B 2008 *J. Am. Chem. Soc.* **130** 3710–1
[32] Poddar P, Morales M B, Frey N A, Morrison S A, Carpenter E E and Srikanth H 2008 *J. Appl. Phys.* **104** 063901
[33] Allia P, Coisson M, Tiberto P, Vinai F, Knobel M, Novak M A and Nunes W C 2001 *Phys. Rev.* B **64** 144420
[34] Denardin J C, Brandl A L, Knobel M, Panissod P, Pakhomov A B, Liu H and Zhang X X 2002 *Phys. Rev.* B **65** 064422
[35] Yamamoto K, Majetich S A, McCartney M R, Sachan M, Yamamuro S and Hirayama T 2008 *Appl. Phys. Lett.* **93** 082502